



## Original Article

# Long term observation of *de novo* adipogenesis using novel bioabsorbable implants with larger size in a porcine model

Shuichi Ogino <sup>a,\*</sup>, Atsushi Yamada <sup>b</sup>, Takashi Nakano <sup>c</sup>, Sunghee Lee <sup>c</sup>, Hiroki Yamanaka <sup>c</sup>, Itaru Tsuge <sup>c</sup>, Yoshihiro Sowa <sup>c</sup>, Michiharu Sakamoto <sup>c</sup>, Fukazawa Kyoko <sup>d</sup>, Yusuke Kambe <sup>d</sup>, Yuki Kato <sup>e</sup>, Jun Arata <sup>a</sup>, Koji Yamauchi <sup>e</sup>, Tetsuji Yamaoka <sup>d</sup>, Naoki Morimoto <sup>c</sup>

<sup>a</sup> Department of Plastic and Reconstructive Surgery, Shiga University of Medical Science, Seta Tsukinowa-cho, Otsu, Shiga 520-2192, Japan

<sup>b</sup> Department of Research and Development for Innovative Medical Devices and Systems, Shiga University of Medical Science, Seta Tsukinowa-cho, Otsu, Shiga 520-2192, Japan

<sup>c</sup> Department of Plastic and Reconstructive Surgery, Graduate School of Medicine, Kyoto University, 54 Shogoin, Kawahara-cho, Sakyou-ku, Kyoto 606-8507, Japan

<sup>d</sup> Department of Biomedical Engineering, National Cerebral and Cardiovascular Center Research Institute, 6-1 Kishibe Shin-machi, Suita, Osaka 564-8565, Japan

<sup>e</sup> Gunze QOL Research Center Laboratory, 1 Zeze, Aono-cho, Ayabe, Kyoto 623-0051, Japan

## ARTICLE INFO

## Article history:

Received 22 December 2022

Received in revised form

27 July 2023

Accepted 13 August 2023

## Keywords:

Adipogenesis

Adipose tissue

Animals

Bioabsorbable materials

Regeneration

## ABSTRACT

**Introduction:** The regeneration of adipose tissue in patients after breast cancer surgery would be desirable without the use of growth factors or cells to avoid potential recurrence and metastasis. We reported that prolate spheroidal-shaped poly-L-lactic acid (PLLA) mesh implants of approximately 18-mm polar diameter and 7.5-mm greatest equatorial diameter containing collagen sponge (CS) would be replaced by regenerated adipose tissue after implantation, thereby suggesting an innovative method for breast reconstruction. Our study aimed to evaluate the adipose tissue regeneration ability of implant aggregates in a porcine model.

**Methods:** We prepared implant aggregates consisting of thirty PLLA mesh implants containing CS packed in a woven poly (glycolic acid) bag. The implant aggregates were inserted under the mammary glands in the porcine abdomen for a year. Single and double groups were classified by inserting either one or two implant aggregates on each side of the abdomen, respectively.

**Results:** In both groups, the volume of the implant aggregates decreased over time, and the formation of adipose tissue peaked between 6 and 9 months. Histologically, the formation of adipose tissue was confirmed in the area that was in contact with native adipose tissue.

**Conclusions:** Our implant aggregates could induce the autologous adipose tissue after long term implantation *in vivo*, without the use of any growth factor or cell treatment, presenting a potential novel method of breast reconstruction.

© 2023, The Japanese Society for Regenerative Medicine. Production and hosting by Elsevier B.V. This is an open access article under the CC BY-NC-ND license (<http://creativecommons.org/licenses/by-nc-nd/4.0/>).

**Abbreviations:** ASCs, adipose-derived stromal cells; PLLA, poly-L-lactic acid; CS, collagen sponge; PGA, poly (glycolic acid); MRI, magnetic resonance imaging; H&E, hematoxylin-eosin; AZAN, azocarmine and aniline blue; BSA, bovine serum albumin; PBS, phosphate-buffered saline.

\* Corresponding author.

**E-mail addresses:** [sogino12@belle.shiga-med.ac.jp](mailto:sogino12@belle.shiga-med.ac.jp) (S. Ogino), [ayamada@belle.shiga-med.ac.jp](mailto:ayamada@belle.shiga-med.ac.jp) (A. Yamada), [evolve@kuhp.kyoto-u.ac.jp](mailto:evolve@kuhp.kyoto-u.ac.jp) (T. Nakano), [nami0128@kuhp.kyoto-u.ac.jp](mailto:nami0128@kuhp.kyoto-u.ac.jp) (S. Lee), [ymnkahrk@kuhp.kyoto-u.ac.jp](mailto:ymnkahrk@kuhp.kyoto-u.ac.jp) (H. Yamanaka), [itsuge@kuhp.kyoto-u.ac.jp](mailto:itsuge@kuhp.kyoto-u.ac.jp) (I. Tsuge), [sowawan@kuhp.kyoto-u.ac.jp](mailto:sowawan@kuhp.kyoto-u.ac.jp) (Y. Sowa), [dojis@kuhp.kyoto-u.ac.jp](mailto:dojis@kuhp.kyoto-u.ac.jp) (M. Sakamoto), [k.fukazawa@ncvc.go.jp](mailto:k.fukazawa@ncvc.go.jp) (F. Kyoko), [kambey698@affrc.go.jp](mailto:kambey698@affrc.go.jp) (Y. Kambe), [yuuki.kato@gunze.co.jp](mailto:yuuki.kato@gunze.co.jp) (Y. Kato), [arata@belle.shiga-med.ac.jp](mailto:arata@belle.shiga-med.ac.jp) (J. Arata), [koji.yamauchi@gunze.co.jp](mailto:koji.yamauchi@gunze.co.jp) (K. Yamauchi), [yamtet@ncvc.go.jp](mailto:yamtet@ncvc.go.jp) (T. Yamaoka), [mnaoki22@kuhp.kyoto-u.ac.jp](mailto:mnaoki22@kuhp.kyoto-u.ac.jp) (N. Morimoto).

Peer review under responsibility of the Japanese Society for Regenerative Medicine.

<https://doi.org/10.1016/j.reth.2023.08.004>

2352-3204/© 2023, The Japanese Society for Regenerative Medicine. Production and hosting by Elsevier B.V. This is an open access article under the CC BY-NC-ND license (<http://creativecommons.org/licenses/by-nc-nd/4.0/>).

## 1. Introduction

The reconstruction of soft tissues to repair deformities caused by trauma, oncologic resection, and congenital disease is challenging. Recently, the demand for breast reconstruction in patients after breast cancer surgery has been increasing. Currently, breast reconstruction approaches include the use of autologous flap, silicone implants, filler injection, or autologous fat injection to replace the lost volume. Despite the success of these methods, some unsolved issues, such as donor site morbidity, volume loss over time [1–3], and development of breast implant-associated anaplastic large cell lymphoma [4], remain. Therefore, new potential methods for the restoration of breast volume are urgently required.

This study aimed to present a novel breast reconstruction strategy for patients after breast cancer surgery. The progress in tissue engineering have enabled the regeneration of adipose tissue using cells, growth factors, and scaffolds [5–10]. The safety of treatment with growth factors or cells, such as adipose-derived stromal cells (ASCs), has not yet been confirmed in patients with breast cancer, owing to the possible induction of tumor proliferation and metastasis [11–15]. Alternative approaches using scaffolds without the addition of cells and growth factors are emerging as a promising solution [16]. In addition, scaffolds are made biocompatible with the target tissue and are also cost-effective [17,18], without the typical manufacturing hurdles seen in cell therapies [19]. The development of scaffolds for adipose tissue regeneration requires controlled biomechanical cues for achieving an appropriate environment, which promote the differentiation of ASCs towards adipogenesis [20]. For example, ASCs cultured on soft hydrogels, mimicking the stiffness of adipose tissue (2 kPa), showed a significant upregulation of adipogenic markers *in vitro* [21]. Since mechanical force is known to affect adipogenesis, *in vitro* studies reported the adipogenesis of ASCs to be inhibited by mechanical compressive force [22] or mechanical stretch [23]. Previously, we had reported that using certain materials to protect the internal space from surrounding tissue pressure can induce regeneration of adipose tissue *in vivo* [24,25].

We had earlier developed an innovative breast reconstruction method using a bioabsorbable implant that is substituted by newly formed adipose tissue after implantation without the use of growth factors or cells [24,25]. The implant consisted of a poly-L-lactic acid (PLLA) mesh containing collagen sponge (CS). Maintenance of the internal space *in vivo* for approximately one year after implantation was essential for the successful formation of adipose tissue from the PLLA implant in the rodent model [24]. However, the amount of adipose tissue formed in rodent and rabbit models was not sufficient to fill the volume required for breast augmentation after clinical mastectomy [24,25]. In a subsequent study [26], we produced implant aggregates consisting of PLLA mesh implants containing CS in a poly (glycolic acid) (PGA) woven bag, which were able to regenerate adipose tissue 6 months after implantation. Magnetic resonance imaging (MRI) was deemed an appropriate method for evaluating the volume of the implant aggregate and formation of adipose tissue in a porcine model.

In this study, we inserted a PLLA implant aggregate of large volume enveloped with a PGA mesh bag into the abdomen, under the mammary gland, of a porcine model for a long duration (one year), and evaluated the regeneration ability of the adipose tissue over this time.

## 2. Methods

### 2.1. Preparation of the bioabsorbable implant aggregates

Prolate spheroidal-shaped PLLA mesh implants containing CS (PELNAC®, Gunze Ltd., Tokyo, Japan) were prepared as reported

previously [24]. Each columnar mesh, 1 cm in diameter and 1 cm in height, was knitted using a 2–0 PLLA thread supplied by Gunze Ltd. One side of the PLLA mesh was closed with purse-string sutures. After tight packing with a 40 mm × 20 mm × 3 mm CS, with a porosity of 80–95%, the other side of the mesh was closed with purse-string sutures as well. The PLLA mesh implants containing CS were approximately 18 mm in polar diameter and 7.5 mm in greatest equatorial diameter, with multiple square openings of 1.5 mm on each side.

Next, as reported previously [26], PGA multifilaments, formed by combining twelve PGA monofilaments with a thickness of 0.015 mm, were woven into an envelope-shaped bag. Eighteen flat woven PGA bags with a dimension of 110 mm × 35 mm were prepared. Thirty implants were packed into each PGA woven bag, resulting in a cylindrical implant aggregate with a diameter of 2.4 cm and a height of 9.0 cm (Fig. 1a). Two untied implant aggregates were used for one minipig of the single group. For the other minipigs, both sides of the implant aggregate were tied up to create a bulge with 4–0 nylon sutures (Diadem: Wondermarks Inc., Tokyo, Japan), resulting in sixteen implant aggregates with a prolate-spheroidal shape, polar radius of approximately 7.0 cm, and the greatest equatorial radius of approximately 2.6 cm (Fig. 1b).

### 2.2. Animal experiments

#### 2.2.1. Experimental design and operative procedure

Minipigs were selected for this study, owing to their large body surface area and skin similar to that of humans. Six female CLAWN miniature swine were purchased from Kagoshima Miniature Swine Research Center (Kagoshima, Japan). Three were used for the single group while the other three were used for the double group. After more than 1 week of acclimatization, 10–11-month-old minipigs weighing between 25.8 and 32.0 kg were used in this study. The animals were cared for as outlined in the Public Health Services Policy on Humane Care and Use of Laboratory Animals, and their general symptoms were assessed daily.

The minipigs were fasted overnight before the administration of general anesthesia. Briefly, the minipigs were sedated via intramuscular injection of 25 mg/kg ketamine (KETALAR®, DAIIICHI

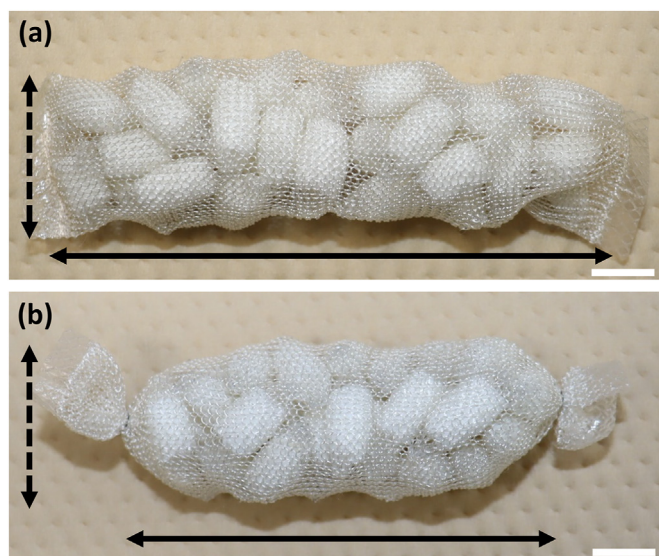


**Fig. 1.** Poly-L-lactic acid implant aggregates. (a) Gross appearance of the poly-L-lactic acid (PLLA) implant aggregates before both sides are tied up. (b) Gross appearance of the PLLA implant aggregates after both sides are tied up. The dashed black arrow indicates the largest diameter of the short axis, and the solid black arrow indicates the greatest length of the long axis. Scale bar: 1 cm.

SANKYO Co., Ltd., Tokyo, Japan) and 0.02 mg/kg medetomidine (DOMITOR®, Nippon Zenyaku Kogyo Co., Ltd., Fukushima, Japan). Then, a peripheral intravenous line and endotracheal tube were inserted. While the minipigs' oxygen saturation was monitored, they were anesthetized by the inhalation of a mixture of air and oxygen containing 2.0–2.5% isoflurane. The abdominal region of the minipig was shaved, and then a 6-cm midline incision was made in the abdomen 1 cm caudal to the umbilicus (Fig. 2). Next, the fat tissue was incised, and a pocket was prepared over the fascia and under the mammary gland on each side of the abdomen. In the single group, one untied implant aggregate was inserted on each side for one of the minipigs, and one tied implant aggregate inserted on each side for two of the minipigs. In the double group, two tied implant aggregates were inserted on each side for all three minipigs. After implantation, both fat and skin were closed with 2-0 blade nylon sutures (Nurolon: Johnson & Johnson K.K., Tokyo, Japan).

### 2.2.2. Evaluation of the implant aggregates

The tissue regeneration inside the implant aggregates were evaluated using ultrasound and MRI under general anesthesia, prior to implantation, immediately after implantation, and 3, 6, 9, and 12 months after implantation. Tissue specimens were harvested approximately 1 cm from the outer edge of the implant aggregate and from just below the skin, up to and including the fascia in contact with the implant aggregate. Tissue samples from the right side of the abdomen were harvested under general anesthesia 6 months after implantation, whereas those from the left side of the abdomen were harvested under general anesthesia 12 months after implantation, subsequently followed by sacrifice of the animal.

**2.2.2.1. Ultrasonography.** Tissue formation inside the implant aggregates was evaluated using an ultrasonographic system (ACUSON S2000 HELX Evolution: Siemens Healthcare K.K., Tokyo, Japan) with a 9L4 probe.

**2.2.2.2. MRI.** As reported previously [26], the minipigs were first placed in a supine position on the examination table. The abdominal area of the minipigs was scanned using a wide-bore 3 T (T) MRI scanner (Magnetom Verio Dot, Siemens Healthcare, Erlangen, Germany) with a dedicated 4-channel large flex coil. The images were scanned in the transverse plane using 3D T1-weighted gradient-echo 2-point Dixon imaging (TR/TE = 5.26/2.46 ms; flip angle = 10°; acquisition matrix = 352 × 172; field of view (FOV) = 285 × 350 mm<sup>2</sup>; slice thickness = 1.0 mm). To acquire each TE image, this Dixon imaging method additionally calculated fat-

only images. The breath was controlled by intravenous injection of 0.4 mg/kg rocuronium bromide (ESLAX®, MSD K.K., Tokyo, Japan) during scanning. The volume of the implant aggregate and of the newly formed adipose tissue inside the implant aggregate were quantified using 3D Slicer [27], a software package for the analysis of medical images.

**2.2.2.3. Histological assessment of the newly formed tissue inside the implant aggregate.** As reported previously [26], the harvested specimens were fixed using 4% paraformaldehyde phosphate buffer solution (FUJIFILM Wako Pure Chemical Corporation, Osaka, Japan). Thereafter, they were equally divided into four blocks along the long axis of the implant aggregates. The second block from the caudal side was embedded in optimum cutting temperature compound (Sakura Fine Technical Co. Ltd., Tokyo, Japan) and frozen using ethanol dry ice. The 16- $\mu$ m-thick frozen section from the central region of the tissues was prepared for Oil Red O staining. The three remaining blocks were paraffin-embedded. Five-micron-thick sections from three aspects of the specimen were used for the hematoxylin-eosin (H&E) and the azocarmine and aniline blue (AZAN) staining, and 5- $\mu$ m-thick sections from the central aspects of the specimen were used for immunohistochemical staining.

All microphotographs were captured using a light microscope (IX83; Olympus Corporation, Tokyo, Japan) at 40 × magnification. For the microphotographs of the H&E-stained sections, the newly formed tissues and the newly formed adipose tissues inside the implant aggregates were evaluated using ImageJ software version 1.53 s (National Institutes of Health, Bethesda, Maryland, USA). The average area for the three aspects of each specimen was used for statistical analysis of the newly formed tissue and newly formed adipose tissue inside each implant aggregate.

**2.2.2.4. Evaluation of the newly formed adipose tissue and capillaries using immunohistochemical staining.** Immunohistochemical staining of Perilipin-1 and CD31 was performed to evaluate the newly formed adipose tissue and capillaries in the newly formed tissue, as per a previous study [26]. After deparaffinization and rehydration, the paraffin sections were incubated in diluted target retrieval solutions (415211; Nichirei Biosciences Inc., Tokyo, Japan) for 20 min at 98 °C. The sections were cooled to 20 °C and rinsed with distilled water. To block endogenous peroxidase activity, the sections were immersed in 3% hydrogen peroxide (FUJIFILM Wako Pure Chemical Industries, Ltd.) and methanol (FUJIFILM Wako Pure Chemical Industries, Ltd.) for 10 min. Thereafter, the sections were once again rinsed with distilled water, and then with 50 mM Tris-HCl buffered saline (Takara Bio Inc., Kusatsu, Japan) with 0.05% Tween 20 (FUJIFILM Wako Pure Chemical Industries Ltd.) and 0.15 M NaCl (TBST). To block nonspecific protein binding, 3% bovine serum albumin (BSA) diluted with phosphate-buffered saline (PBS) was applied for 60 min at 20 °C. For the immunohistochemical staining of Perilipin-1, the primary antibody (Perilipin-1 [D1D8] XP Rabbit mAb #9349; Cell Signaling Technology, Inc., Danvers, MA, USA) was applied at a dilution of 1:2000 using 1% BSA in PBS and incubated overnight at 4 °C. For the immunohistochemical staining of CD31, the primary antibody (anti-CD31 antibody [EPR17259] rabbit mAb #ab182981; Abcam plc., Tokyo, Japan) was applied at a dilution of 1:10000 using 1% BSA in PBS and incubated overnight at 4 °C. After rinsing the sections with TBST, a peroxidase-labeled secondary antibody (rabbit anti-goat simple stain MAX PO [R]; Histofine; Nichirei Biosciences Inc.) was applied for 30 min at 20 °C. After rinsing with TBST once more, the sections were exposed to 3,3'-diaminobenzidine tetrahydrochloride (Dako Japan Co., Ltd., Tokyo, Japan) for 5 min at 20 °C and counterstained with hematoxylin. All microphotographs were captured using a light microscope (IX83; Olympus Corporation) at 40 × magnification.

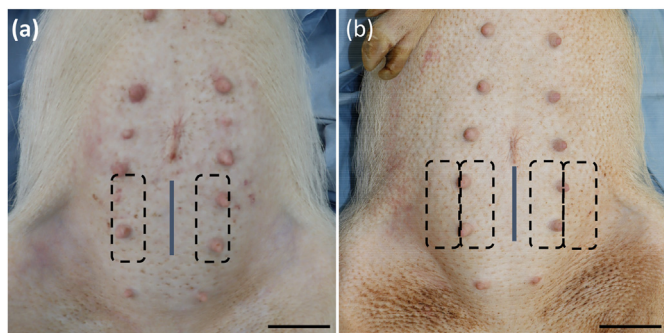


**Fig. 2.** Areas into which the implant aggregates were inserted. (a) Insertion area in the single group. (b) Insertion area in the double group. The gray line represents the 6-cm incision. The black dotted area shows where the implant aggregates were inserted. Scale bar: 5 cm.

### 2.3. Statistical analysis

Statistical significance was evaluated by analysis of variance and the Tukey–Kramer test. All data are expressed as mean  $\pm$  standard deviation. Statistical significance was set at a  $p$  value  $< 0.05$ . Microsoft Excel with the Statcel 4 software add-in (OMS Publishing Inc., Tokyo, Japan) was used for all statistical analyses.

## 3. Results

Tissue samples from the right and left sides were harvested 6 and 12 months after implantation, respectively. During the follow-up period, no infection or tumor formation was observed around the implant aggregates. However, one minipig in the double group died from emaciation at 8 months after implantation, a result deemed unrelated to the implants. Therefore, the number of MRI results at 9 and 12 months and the number of histological assessments at 12 months decreased by two.

### 3.1. Ultrasonographic findings

The ultrasonographic findings of the implant aggregates are shown in Fig. 3. Immediately after implantation, in both the groups, the outer surfaces of the implant aggregates were hyperechoic and clearly defined. In contrast, ultrasonic observation inside the implant aggregate was unclear due to the presence of PLLA thread and PGA mesh. At 3, 6, 9, and 12 months after implantation, the definite outer surface of the implant aggregate disappeared in both the groups, and a hyperechoic area was identified on the skin side of the implant aggregates. Observation of the deep fascial side of the implant aggregates was not possible. In this study, ultrasonic observation was determined to be inappropriate for the proper evaluation of the implant aggregates.

### 3.2. MRI findings

The MRI scans are shown in Fig. 4. The outer edge of the implant aggregate was easily observed at all time points in both the groups. Newly formed adipose tissue was identified as a high-intensity lesion within the implant aggregate. In both the groups, the formation of adipose tissue inside the implant aggregate was confirmed starting 3 months after implantation, particularly on the skin side where it was in contact with the surrounding fat.

The time course in the volumes of the implant aggregates and newly formed adipose tissue inside the implant aggregates is shown

in Fig. 5. The volume of the implant aggregates gradually decreased in a statistically significant manner over time. The volumes of the implant aggregates in the single and double groups at 12 months after implantation were 33.9% and 32.4%, respectively, of those immediately post-implantation. The volume of the newly formed adipose tissue inside the implant aggregates reached a maximum at 6 months for the single group and 9 months for the double group after implantation, decreasing at 12 months. The percentage of the newly formed adipose tissue in the implant aggregates reached a maximum at 9 months in the single and double groups, being 28.3% and 35.2%, respectively and decreased at 12 months.

### 3.3. Histological assessment of the newly formed tissue

Micrographs of the H&E-stained, Oil Red O-stained, AZAN-stained, and anti-perilipin-stained sections are shown in Fig. 6a, b, c and 7a, respectively. The areas of the newly formed adipose tissues measured on the H&E sections are shown in Table 1. The continued presence of the PLLA mesh was confirmed histologically at all time points in both the groups. At 6 months after implantation, in both the groups, the internal space of the implant aggregates was maintained, and the newly formed tissue inside the implant aggregates consisted of both adipose tissue and collagen fibers. Most of the adipose tissue was regenerated in the area that was in contact with the native adipose tissue on the skin side, and the regeneration occurred for each unit of PLLA mesh implant within the aggregate. A small amount of adipose tissue was regenerated on the fascial side of the implant, an area in no contact with native adipose tissue. At 12 months, the distance between the PLLA threads became narrower in both groups, the area of the newly formed tissues decreased, and the internal space was no longer maintained. Furthermore, the amount of newly regenerated adipose tissue was not retained and decreased to some extent. The percentage of newly formed adipose tissue in the newly formed tissue at 6 months was significantly higher in the single group than in the double group ( $p < 0.05$ ).

### 3.4. Evaluation of capillary formation inside the implant aggregate

Micrographs of the anti-CD31-stained sections are shown in Fig. 7b. At 6 months, in both groups, evenly dispersed capillary formation was observed in the newly formed adipose tissue as well as in the formed collagen fibers. At 12 months, in both the groups, most of the newly formed capillaries were observed around the threads.

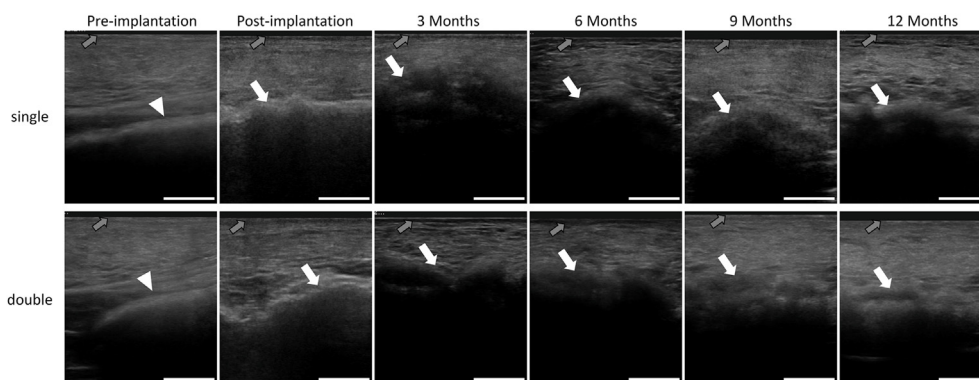


**Fig. 3.** Ultrasound evaluation inside the implant aggregate. The representative ultrasound images of the single group indicate the use of implant aggregates tied at both ends. In both the groups, the ultrasonic observation inside the implant aggregate was unclear due to the PLLA thread and PGA mesh after implantation. The white arrowhead indicates the deep fascia. White arrows indicate the outer surface of the implant aggregates. Gray arrows indicate the skin surface. Scale bar: 1 cm. PLLA, poly-L-lactic acid; PGA, poly (glycolic acid).

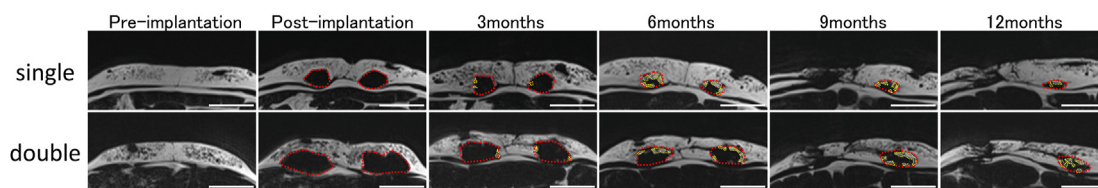


**Fig. 4.** Magnetic resonance imaging of the implant aggregates and the newly formed adipose tissue. The representative magnetic resonance imaging of the single group indicate the use of implant aggregates tied at both ends. In both groups, the area of the implant aggregates gradually decreased over time. The newly formed adipose tissue was identified as a hyperintense lesion in the Dixon fat-only images after 3 months. The red dotted lines indicate the area of the implant aggregate, and the yellow dotted lines indicate the area of the newly formed adipose tissue. Scale bar: 5 cm.

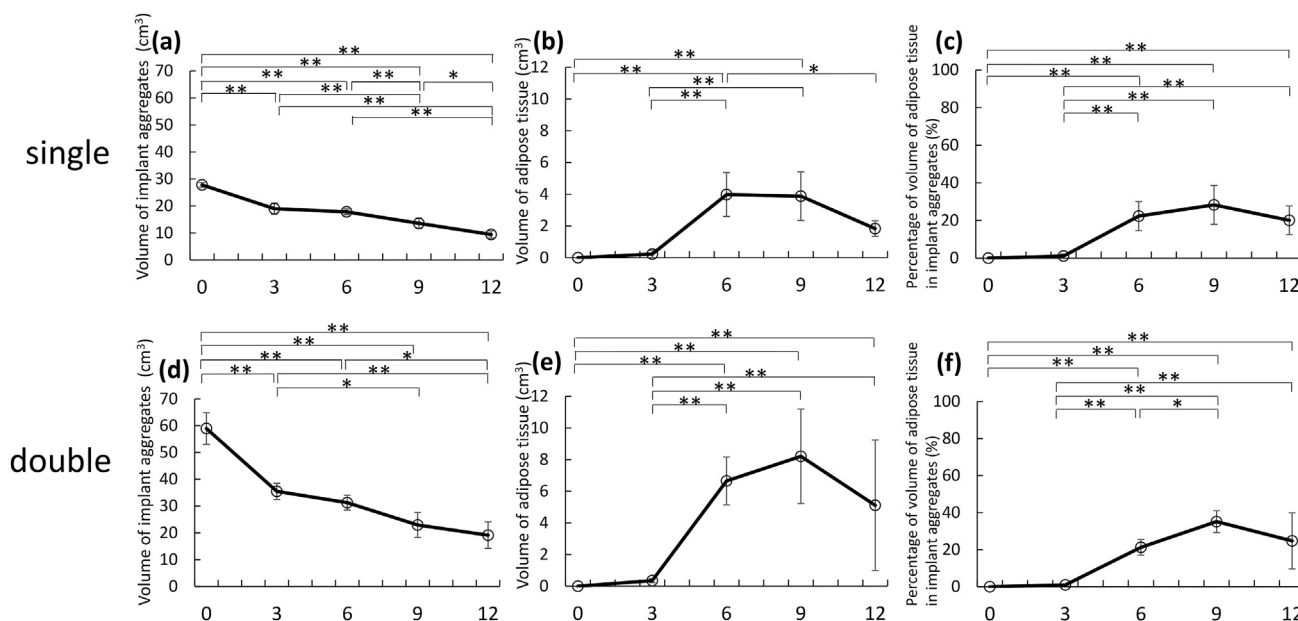


**Fig. 5.** Time course of the volumes of the implant aggregates and newly formed adipose tissue inside the implant aggregates using magnetic resonance imaging. (a, d) Time course of the volume of the implant aggregates. The volume decreased over time in both the groups. (b, e) Time course of the volume of adipose tissue inside the implant aggregates. The volume reached a maximum at 6 months in the single group and 9 months in the double group. (c, f) Percentage of the volume of adipose tissue with respect to that of the implant aggregates. The percentage reached a maximum at 9 months in both the groups. (a), (b), and (c) indicate the single group, and (d), (e), and (f) indicate the double group. In the single group, 0, 3, 6 (n = 6), 9, and 12 months (n = 3) were the time points. In the double group, 0, 3, 6 (n = 6), 9, and 12 months (n = 2) were the time points. Data are presented as the mean ± standard deviation. \*p < 0.05, \*\*p < 0.01.

#### 4. Discussion

In this study, we observed adipogenesis using two models of our implant aggregates over a long duration of one year, confirming that our implant aggregates can regenerate adipose tissue. MRI was an appropriate method for evaluating the volumes of the implant aggregates and regenerated adipose tissue over time. However, the implant aggregates were unable to maintain the regenerated adipose tissue beyond a year.

In a previous study [26], we investigated the efficacies of 3D surface imaging, ultrasonography, and MRI as evaluation methods of adipogenesis inside implant aggregates over time using a porcine model. While MRI was the most appropriate method for studying adipogenesis, ultrasonography was also highly potent. In our study on rabbits [28], we confirmed the formation of adipose tissue inside a polypropylene mesh containing CS using ultrasound imaging one year after implantation. Another study showed that PLLA in PBS at 37 °C was degraded to 50% (by weight) within 2 years, and PGA was completely degraded within 2–3 months [29]. In the present study, complete dissolution of PLLA was not histologically confirmed (Fig. 6). Therefore, ultrasonography may not be an appropriate method for evaluating adipose tissue, owing to the difficulty of accurately determining the hyperechoic area and observing the

fascial side of the implant aggregate at all time points (Fig. 3). This difference in the ultrasonography results between our rabbit [28] and the present minipig studies may be attributed to the difference in the size, shape, and material of the implants used. Therefore, in the current study, MRI was proven to be a superior evaluation method for the area inside the implant aggregate over time.

In terms of the adipose tissue regeneration ability of our implant aggregates, they were found to promote the formation of adipose tissue at 6 months, which was then retained until 9 months (Figs. 4, 5b and e, and Table 1). Maintaining the internal space using materials able to withstand the *in vivo* tissue compressive forces for months leads to the regeneration of adipose tissue [30–32]. Considering the relationship between the *in vivo* tissue pressure and adipose tissue formation, pre-breast expansion using an external soft tissue expander could enable the transfer of large volumes of fat safely and effectively with a very high survival rate [33]. Methods using intratissular expansion and serial fat grafting have been shown to achieve an aesthetically pleasant and stable breast mound [34]. Therefore, generating an internal space in advance is an important factor for adipose tissue grafting to avoid tissue pressure. Moreover, maintenance of the internal space for over a year is the most important factor for adipogenesis [24,25]. In the present study, our implant aggregates maintained the internal

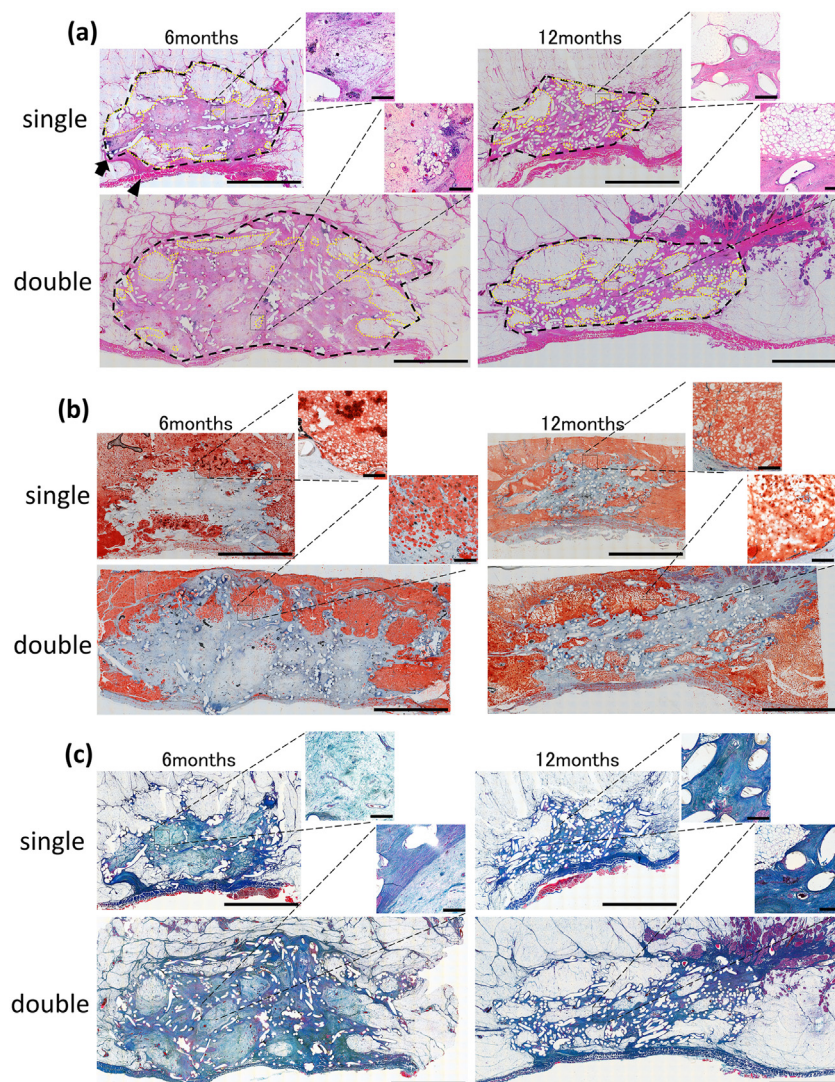


**Fig. 6.** Histological evaluation of the implant aggregates. (a) Light micrographs of the hematoxylin-eosin (H&E)-stained sections, (b) light micrographs of the Oil Red O-stained sections, and (c) light micrographs of the azocarmine and aniline blue (AZAN)-stained sections. The representative histological images of tissue from the single group indicate the use of implant aggregates tied at both ends. The presence of poly-L-lactic acid (PLLA) threads was confirmed at all time points in both groups. The internal space in the implant aggregate was maintained until 6 months and had collapsed by 12 months. At 6 months, most of the newly formed adipose tissue was observed on the skin side. At 12 months, the regenerated adipose tissue remained to some extent. The black dotted lines indicate the area of newly formed tissue inside the implant aggregates, and the yellow dotted lines indicate the areas of newly formed adipose tissue. The arrowhead indicates the fascia, and the solid arrow indicates the PLLA thread. Scale bar: 10 mm; magnified scale bar: 0.5 mm.

space to some extent, until nine months after implantation (Fig. 5). Therefore, up until that point, they could contribute to the regeneration of the adipose tissue by reducing the compressive force of the surrounding tissue.

Regarding the mechanism of adipogenesis, previous studies reported that, in a model where an arteriovenous bundle or arteriovenous shunt loop was placed in a porous chamber, adipose tissue formation occurred both from the porous area in contact with the native adipose tissue and perivascular area placed in the chamber [35–37]. Both the histological and MRI findings in our present study showed that, at 6 months, the adipose tissue was mainly regenerated inside the implant aggregates in the area in contact with the native adipose tissue (Figs. 4, 6a, b and 7a), and the newly formed capillaries regenerated evenly, as shown in Fig. 7b. In addition, the formation of adipose tissue in the double group was slower than that in the single group, owing to the difference in the extent of contact with native adipose tissue (Table 1). Therefore, the contact with the native adipose tissue is important factor for adipogenesis using our implants. Thus, we suggest that the main target

for our implants is patients undergoing partial mastectomy so that the implant is able to have more contact with the surrounding fat. However, our implant aggregates were not able to maintain the internal space until the adipose tissue was regenerated around the newly formed capillaries or from the area in contact with the regenerated adipose tissue inside the fascial-side implant.

The objective of this study was to regenerate a large volume (>100 ml) of fat, which is considered clinically necessary for breast reconstruction after mastectomy. Prior to achieving this, investigation of the correlation between the volumes of implant aggregate and newly formed adipose tissue is important and necessary. Large volumes of adipose tissue has been regenerated via autologous fat transfer using bioabsorbable polycaprolactone-based scaffolds in a porcine model [38] as well as poly-4-hydroxybutyrate mesh scaffolds [39]. However, methods requiring autologous fat grafting involve donor site morbidity. Our implant aggregates could be conveniently inserted multiple times as necessary, in varying amounts depending on the situation, without the addition of cells or growth factors, and without little risk of morbidity.

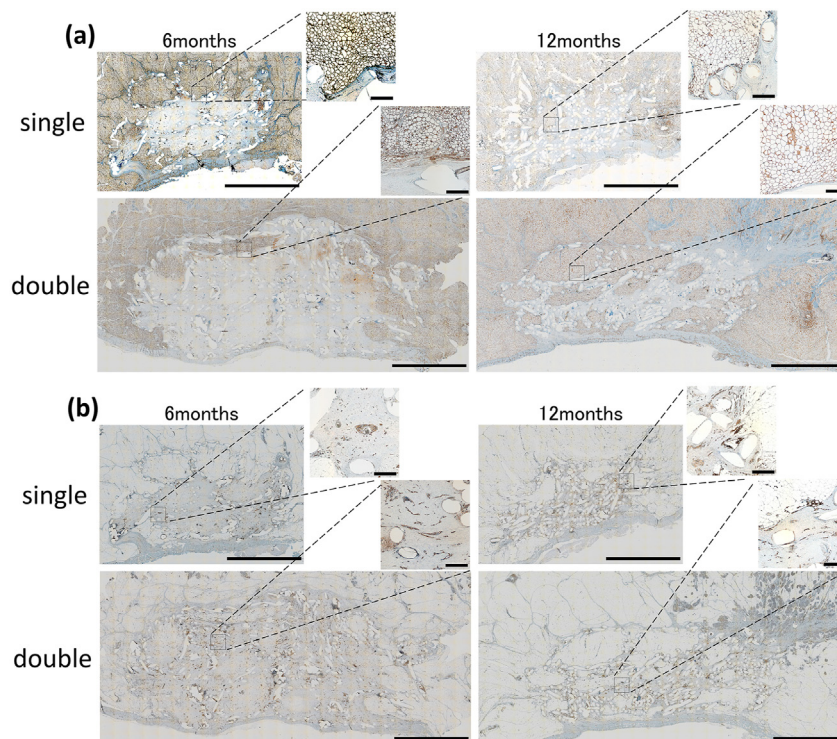


**Fig. 7.** Immunohistochemical evaluation of the implant aggregates. (a) Light micrographs of anti-Perilipin-1-stained sections. At 6 months, regeneration of adipose tissue on the skin side was confirmed. At 12 months, the regenerated adipose tissue remained to some extent. (b) Light micrographs of anti-CD31-stained sections. Newly formed capillaries were observed both in the areas of newly formed adipose tissue and in the areas of formed collagen fibers at 6 months in both the groups. At 12 months, most of the newly formed capillaries were observed around the threads. The representative immunohistochemical images of the single group indicate use of implant aggregates tied at both ends. Scale bar: 10 mm; magnified scale bar: 0.5 mm.

**Table 1**  
Evaluation of the newly formed tissue and newly formed adipose tissue inside the implant aggregates.

	Time after implantation			
	6 months		12 months	
	Single group (n = 3)	Double group (n = 3)	Single group (n = 3)	Double group (n = 2)
Area of the newly formed tissue (mm <sup>2</sup> )	194.6 ± 22.4	452.2 ± 30.3	121.9 ± 10.0	250.3 ± 33.5
Area of the newly formed adipose tissue (mm <sup>2</sup> )	80.3 ± 27.7	64.8 ± 20.9	28.4 ± 10.7	77.3 ± 46.5
Percentage of the newly formed adipose tissue in the newly formed tissue (%)	42.4 ± 8.4	14.7 ± 4.1*	23.5 ± 6.6	27.7 ± 13.6

Data are expressed as the mean ± standard deviation. \*p < 0.05 versus the single group at 6 months.

A limitation of this study is that our implant aggregates were unable to retain the newly regenerated adipose tissue beyond a year. This could be due to the increased inflammation and elevation of internal pressure inside the implant aggregates after collapse of the PLLA implant structure, both caused by PLLA absorption. In subsequent studies, we plan to explore the effect of PLLA implants of various shapes on tissue pressure resistance, as well as various implantation methods that may ensure a larger contact area with native adipose tissue, in order to maintain the internal space for more than a year and evaluate the correlation between the volume of the implant aggregate and the newly formed adipose tissue using a porcine model.

**5. Conclusions**

Implant aggregates regenerated the adipose tissue, irrespective of the number of the implant aggregates. The aggregates maintained the internal space and retained the newly formed adipose tissue for up to 9 months. They could induce the autologous adipose tissue after implantation *in vivo*, without the need for

growth factors or cells, thereby suggesting a novel method of breast reconstruction.

**Author contributions**

SO and NM contributed to the study conception and design. YukK and KY prepared the materials, and SO, AY, TN, SL, MS, FK, YusK, YukK, TY, and NM performed the experiments. SO, HY, IT, YS, JA, TY and NM analyzed the data. SO and NM wrote the first draft of the manuscript, and all authors commented on the subsequent versions of the manuscript. All authors have read and approved the final manuscript. SO is the grant recipient of JSPS KAKENHI [grant number JP19K18926] and NM is the grant recipient of AMED [grant number JP19hm0102068].

**Ethics statement**

In this study, the animals were maintained at the Research Center for Animal Life Science, Shiga University of Medical Science. The experimental protocol (permit number: 2019-7-10 (H6)) was

designed in accordance with the ARRIVE guidelines and was approved by the Institutional Animal Care and Usage Committee at Shiga University of Medical Science. In this study, we made all efforts to reduce animal suffering and minimize the number of animals used, in accordance with the protocols established by the Research Center for Animal Life Science of Shiga University of Medical Science.

### Data availability statement

The datasets generated during and/or analyzed during the current study are available from the corresponding author on reasonable request.

### Acknowledgments

This work was partially supported by JSPS KAKENHI [grant number JP19K18926] and AMED [grant number JP19hm0102068]. We would like to thank Khiem Tran Dang and Tohru Tani for providing technical support with the use of general anesthesia, Mayumi Kunimatsu for assistance with the animal experiments, Central Research Laboratory, Shiga University of Medical Science for support in conducting the animal experiments, and Editage (www.editage.com) for English language editing.

### References

- Coleman SR, Saboeiro AP. Fat grafting to the breast revisited: safety and efficacy. *Plast Reconstr Surg* 2007;119:775–85. discussion 86–7.
- Delay E, Garson S, Tousson G, Sinna R. Fat injection to the breast: technique, results, and indications based on 880 procedures over 10 years. *Aesthetic Surg J* 2009;29:360–76.
- Gir P, Brown SA, Oni G, Kashefi N, Mojallal A, Rohrich RJ. Fat grafting: evidence-based review on autologous fat harvesting, processing, reinjection, and storage. *Plast Reconstr Surg* 2012;130:249–58.
- Brody GS, Deapen D, Taylor CR, Pinter-Brown L, House-Lightner SR, Andersen JS, et al. Anaplastic large cell lymphoma occurring in women with breast implants: analysis of 173 cases. *Plast Reconstr Surg* 2015;135:695–705.
- Chang KH, Liao HT, Chen JP. Preparation and characterization of gelatin/hyaluronic acid cryogels for adipose tissue engineering: in vitro and in vivo studies. *Acta Biomater* 2013;9:9012–26.
- Choi JH, Gimble JM, Lee K, Marra KG, Rubin JP, Yoo JJ, et al. Adipose tissue engineering for soft tissue regeneration. *Tissue Eng Part B* 2010;16:413–26.
- Huber B, Borchers K, Tovar GE, Kluger PJ. Methacrylated gelatin and mature adipocytes are promising components for adipose tissue engineering. *J Biomater Appl* 2016;30:699–710.
- Louis F, Kitano S, Mano JF, Matsusaki M. 3D collagen microfibers stimulate the functionality of preadipocytes and maintain the phenotype of mature adipocytes for long term cultures. *Acta Biomater* 2019;84:194–207.
- O'Halloran NA, Dolan EB, Kerin MJ, Lowery AJ, Duffy GP. Hydrogels in adipose tissue engineering-Potential application in post-mastectomy breast regeneration. *J Tissue Eng Regen Med* 2018;12:2234–47.
- Zhu Y, Kruglikov IL, Akgul Y, Scherer PE. Hyaluronan in adipogenesis, adipose tissue physiology and systemic metabolism. *Matrix Biol* 2019;78–79:284–91.
- Alperovich M, Lee ZH, Friedlander PL, Rowan BG, Gimble JM, Chiu ES. Adipose stem cell therapy in cancer reconstruction: a critical review. *Ann Plast Surg* 2014;73(Suppl 1):S104–7.
- Chandler EM, Seo BR, Califano JP, Andresen Eguiluz RC, Lee JS, Yoon CJ, et al. Implanted adipose progenitor cells as physicochemical regulators of breast cancer. *Proc Natl Acad Sci U S A* 2012;109:9786–91.
- Muehlberg FL, Song YH, Krohn A, Piniella SP, Droll LH, Leng X, et al. Tissue-resident stem cells promote breast cancer growth and metastasis. *Carcinogenesis* 2009;30:589–97.
- Rowan BG, Gimble JM, Sheng M, Anbalagan M, Jones RK, Frazier TP, et al. Human adipose tissue-derived stromal/stem cells promote migration and early metastasis of triple negative breast cancer xenografts. *PLoS One* 2014;9:e89595.
- Zhao M, Sachs PC, Wang X, Dumur CI, Idowu MO, Robila V, et al. Mesenchymal stem cells in mammary adipose tissue stimulate progression of breast cancer resembling the basal-type. *Cancer Biol Ther* 2012;13:782–92.
- Gerges I, Tamplenizza M, Martello F, Koman S, Chincarini G, Recordati C, et al. Conditioning the microenvironment for soft tissue regeneration in a cell free scaffold. *Sci Rep* 2021;11:13310.
- Martello F, Gerges I, Tocchio A, Tamplenizza M, Bellezza G. 7 - Bringing bioresorbable polymers to market. In: Perale G, Hilborn J, editors. *Bioresorbable polymers for biomedical applications*. Woodhead Publishing; 2017. p. 133–49.
- Maitz MF. Applications of synthetic polymers in clinical medicine. *Biosurface and Biotribology* 2015;1:161–76.
- Au P, Hursh DA, Lim A, Moos Jr MC, Oh SS, Schneider BS, et al. FDA oversight of cell therapy clinical trials. *Sci Transl Med* 2012;4:149fs31.
- Rossi E, Gerges I, Tocchio A, Tamplenizza M, Aprile P, Recordati C, et al. Biologically and mechanically driven design of an RGD-mimetic macroporous foam for adipose tissue engineering applications. *Biomaterials* 2016;104:65–77.
- Young DA, Choi YS, Engler AJ, Christman KL. Stimulation of adipogenesis of adult adipose-derived stem cells using substrates that mimic the stiffness of adipose tissue. *Biomaterials* 2013;34:8581–8.
- Hossain MG, Iwata T, Mizusawa N, Shima SW, Okutsu T, Ishimoto K, et al. Compressive force inhibits adipogenesis through COX-2-mediated down-regulation of PPARgamma2 and C/EBPalpha. *J Biosci Bioeng* 2010;109:297–303.
- Yang X, Cai X, Wang J, Tang H, Yuan Q, Gong P, et al. Mechanical stretch inhibits adipogenesis and stimulates osteogenesis of adipose stem cells. *Cell Prolif* 2012;45:158–66.
- Ogino S, Morimoto N, Sakamoto M, Jinno C, Yoshikawa K, Enoshiri T, et al. Development of a novel bioabsorbable implant that is substituted by adipose tissue in vivo. *J Tissue Eng Regen Med* 2018;12:633–41.
- Ogino S, Sakamoto M, Lee S, Yamanaka H, Tsuge I, Arata J, et al. De novo adipogenesis using a bioabsorbable implant without additional cells or growth factors. *J Tissue Eng Regen Med* 2020;14:920–30.
- Ogino S, Yamada A, Kambe Y, Nakano T, Lee S, Sakamoto M, et al. Preliminary report of de novo adipogenesis using novel bioabsorbable implants and image evaluation using a porcine model. *J Artif Organs* 2022;25:245–53.
- Fedorov A, Beichel R, Kalpathy-Cramer J, Finet J, Fillion-Robin JC, Pujol S, et al. 3D slicer as an image computing platform for the quantitative imaging network. *Magn Reson Imaging* 2012;30:1323–41.
- Tsuji W, Inamoto T, Ito R, Morimoto N, Tabata Y, Toi M. Simple and long-standing adipose tissue engineering in rabbits. *J Artif Organs* 2013;16:110–4.
- Ikada Y, Tsuji H. Biodegradable polyesters for medical and ecological applications. *Macromol Rapid Commun* 2000;21:117–32.
- Cho SW, Kim SS, Rhie JW, Cho HM, Choi CY, Kim BS. Engineering of volume-stable adipose tissues. *Biomaterials* 2005;26:3577–85.
- Bellas E, Panilaitis BJ, Glettig DL, Kirker-Head CA, Yoo JJ, Marra KG, et al. Sustained volume retention in vivo with adipocyte and lipoaspirate seeded silk scaffolds. *Biomaterials* 2013;34:2960–8.
- Peng Z, Dong Z, Chang Q, Zhan W, Zeng Z, Zhang S, et al. Tissue engineering chamber promotes adipose tissue regeneration in adipose tissue engineering models through induced aseptic inflammation. *Tissue Eng C Methods* 2014;20:875–85.
- Khouiri RK, Eisenmann-Klein M, Cardoso E, Cooley BC, Kacher D, Gombos E, et al. Brava and autologous fat transfer is a safe and effective breast augmentation alternative: results of a 6-year, 81-patient, prospective multicenter study. *Plast Reconstr Surg* 2012;129:1173–87.
- Stillaert FB, Sommeling C, D'Arpa S, Creyten D, Van Landuyt K, Depypere H, et al. Intratissular expansion-mediated, serial fat grafting: a step-by-step working algorithm to achieve 3D biological harmony in autologous breast reconstruction. *J Plast Reconstr Aesthetic Surg* 2016;69:1579–87.
- Yuan Y, Gao J, Ogawa R. Mechanobiology and mechanotherapy of adipose tissue-effect of mechanical force on fat tissue engineering. *Plast Reconstr Surg Glob Open* 2015;3:e578.
- Tanaka Y, Sung KC, Fumimoto M, Tsutsumi A, Kondo S, Hinohara Y, et al. Prefabricated engineered skin flap using an arteriovenous vascular bundle as a vascular carrier in rabbits. *Plast Reconstr Surg* 2006;117:1860–75.
- Tanaka Y, Tsutsumi A, Crowe DM, Tajima S, Morrison WA. Generation of an autologous tissue (matrix) flap by combining an arteriovenous shunt loop with artificial skin in rats: preliminary report. *Br J Plast Surg* 2000;53:51–7.
- Chhaya MP, Balmayer ER, Hutmacher DW, Schantz JT. Transformation of breast reconstruction via additive Biomanufacturing. *Sci Rep* 2016;6:28030.
- Rehnke RD, Schusterman 2nd MA, Clarke JM, Price BC, Waheed U, Debski RE, et al. Breast reconstruction using a three-dimensional absorbable mesh scaffold and autologous fat grafting: a composite strategy based on tissue-engineering principles. *Plast Reconstr Surg* 2020;146. 409e-13e.